Dislocation formation in heavily As-doped Czochralski grown silicon

L. Stockmeier[1], L. Lehmann[2], A. Miller[3], C. Reimann[1,4], J. Friedrich[1,4]

[1] *Fraunhofer THM, Am St.-Niclas-Schacht 13, 09599 Freiberg, Germany*

[2] *Siltronic AG, Berthelsdorfer Straße 113, 09599 Freiberg, Germany*

[3] *Siltronic AG, Johannes-Hess-Straße 24, 84489 Burghausen, Germany*

[4] *Fraunhofer IISB, Schottkystraße 10, 91058 Erlangen, Germany*

Abstract

During the growth of <100>-oriented, heavily n-type doped silicon crystals by the Czochralski method dislocation formation occurs frequently, leading to a reduction of the crystal yield. Up to now, it is not clear where and why the dislocations form. Therefore, heavily As-doped crystals were studied in this work in more detail by means of X-ray tomography (XRT) and synchrotron X-ray tomography (SXRT) and it was possible to localize the origin of the dislocations. From the data obtained it is concluded that dislocations form during growth of the top cone of the crystals in the vicinity of one of the four so-called growth ridges. These growth ridges are a result of the growth of the {111}-facets, which occur at the crystal periphery in the four [110]-directions.

1. Introduction

PowerMOS devices [1] are based on dislocation-free heavily doped silicon crystals which are grown by the Czochralski (CZ) method. It is observed that dislocations form more frequently during the growth of <100>-oriented, heavily n-type doped crystals (>1x10^{19} dopants/cm^3) than of heavily p-type or not heavily doped material [2–6]. The occurrence of dislocations will cause the formation of grain boundaries and result in a so-called “structure loss” [7]. Therefore, dislocations lead to a lower crystal yield, thus dislocation formation has to be prevented. Whether the crystal is dislocation-free or not can be distinguished by the appearance of so-called growth ridges on the surface of the crystal [8]. These growth ridges are a result of the growth of the {111}-facets which occur at the crystal periphery in the four [110]-directions. When dislocations form during the

growth of the crystal, the growth mode of the facets is influenced [9] and as a result the growth ridge changes its form or can even disappear.

It is empirically known that dislocation formation often takes place during growth of the top cone [10] of heavily n-type doped silicon crystals by the CZ method. This is also underlined by the experimental results for the industrial production of <100>-oriented, heavily As-doped 6” (153 mm) Si CZ crystals. In fig. 1 the relative occurrence of an interruption of the growth process is shown, versus the crystal diameter at which the growth runs were stopped due to “structure loss”. As it can be seen clearly in fig. 1, the growth process is stopped frequently during the top cone phase. It is also known that the shape of the top cone affects the risk for dislocation formation [10; 11] and the crystals are therefore typically pulled with an acute top cone.

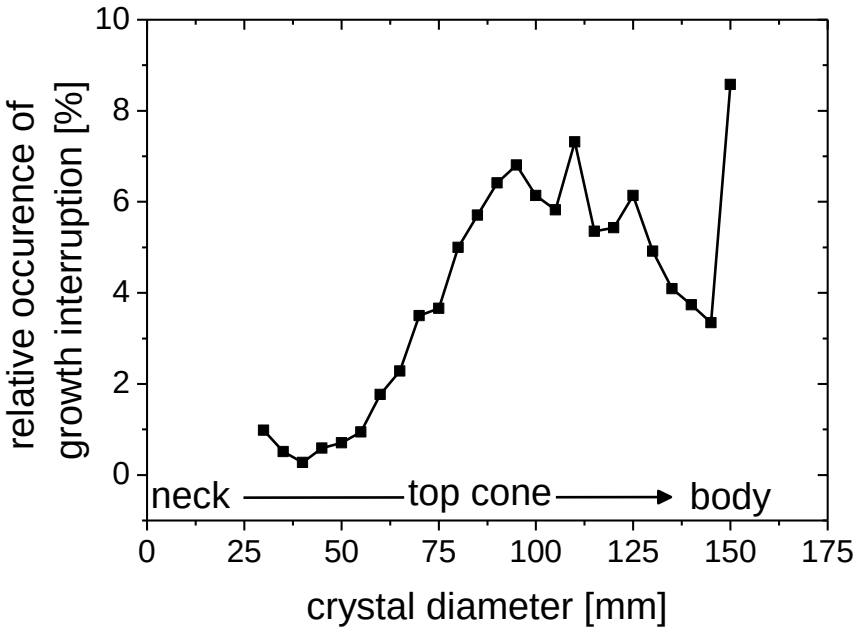

Fig. 1: Frequency of the occurrence of a growth ridge loss in dependence of the crystal diameter at which the crystal growth runs were stopped after the loss of a growth ridge. The data stem from more than 2000 heavily As-doped 6“ CZ crystal growth runs in industrial production.

But, it is still not clear where exactly and also why the dislocations form during the growth process. Therefore, a systematic analysis of the phenomenon of the dislocation formation in heavily As-doped CZ silicon crystals was carried out.

2. Approach

<100> oriented, heavily As-doped CZ silicon crystals targeting diameters of 5” and 6” with an electrical resistivity in the range of 0.002 to 0.004 Ωcm were characterized. Dislocation formation took place during growth of the crystals. The crystal length, at which the loss of the growth ridge occurred, as a result of the dislocation formation, was detected visually. A photograph of such a “growth ridge loss” is shown in fig. 2. A growth ridge can clearly be seen in the top region of fig. 2. Also, the so-called “surface facet” [12] is visible on the crystal surface. In the lower half of the photograph a growth ridge loss appears, affecting the shape of the growth ridge. Later on during the growth process, the growth ridge disappears completely.

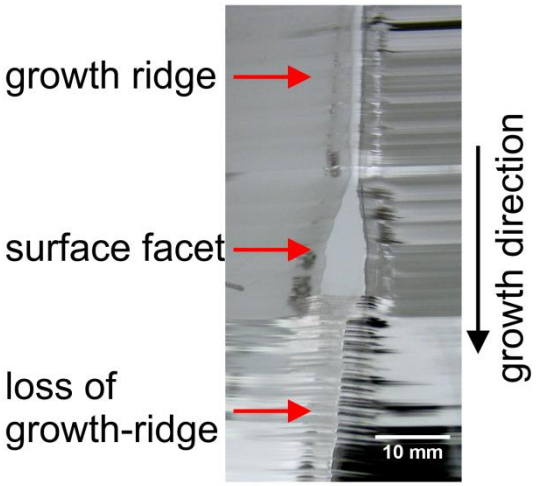

Fig. 2: Photograph of a growth ridge loss, which occurred during the growth of the top cone of a heavily As-doped CZ Si crystal. The growth direction is from top to bottom.

From these dislocated crystals wafers in distances of 10 mm apart from each other were prepared perpendicular to the pulling direction and mechanically polished on both sides. Moreover, one crystal was cut parallel to the growth direction in a {110}-plane, which composed of two growth ridges on opposite sides of the sample. This sample was grinded and polished mechanically to fully compose the two growth ridges within a thickness of 1 mm.

The wafers cut perpendicular and the slab cut parallel to the growth direction were characterized by means of X-ray tomography (XRT). The XRT-measurements were

conducted in transmission mode with the QC-TT system of Bruker, working with a Mo X-ray tube and a detector in transmission mode with a resolution of 80 µm [13].

To characterize the growth ridge loss in more detail another top cone containing a growth ridge loss was cut parallel to the growth direction in a {110}-plane. A sample was prepared from this cut, grinded and polished. This sample was characterized in more detail by synchrotron X-ray tomography (SXRT) at the TOPO/TOMO beamline of the Ångström source Karlsruhe (ANKA) in the Karlsruhe Institute of Technology (KIT) [14]. A reflection-mode setup was used and the area near a growth ridge loss was mapped with SXRT. The sample investigated by SXRT was later chemically etched [15], to analyze the {111}-facets [8; 16] inside of the growth ridge.

3. Results

When dislocations form during the growth of the crystal, they can propagate by different means [17]. A schematic drawing of the propagation of dislocations during the growth of the CZ top cone is shown in fig. 3 for a cross section parallel to the growth direction. The dashed line marks the concave solid-liquid phase boundary during the growth process for the dislocation-free crystal, indicated by “boundary for dislocation-free growth”. When dislocations form they can propagate back into the beforehand dislocation-free crystal on their designated glide systems. The distance dislocations can propagate back into the beforehand dislocation-free silicon crystal is usually half the crystal diameter [18]. The ongoing growth of the crystal, indicated by the dotted line, leads to so-called “growth dislocations”. These dislocations can multiply, resulting in polycrystalline growth. A similar propagation of dislocations is described in [17; 19].

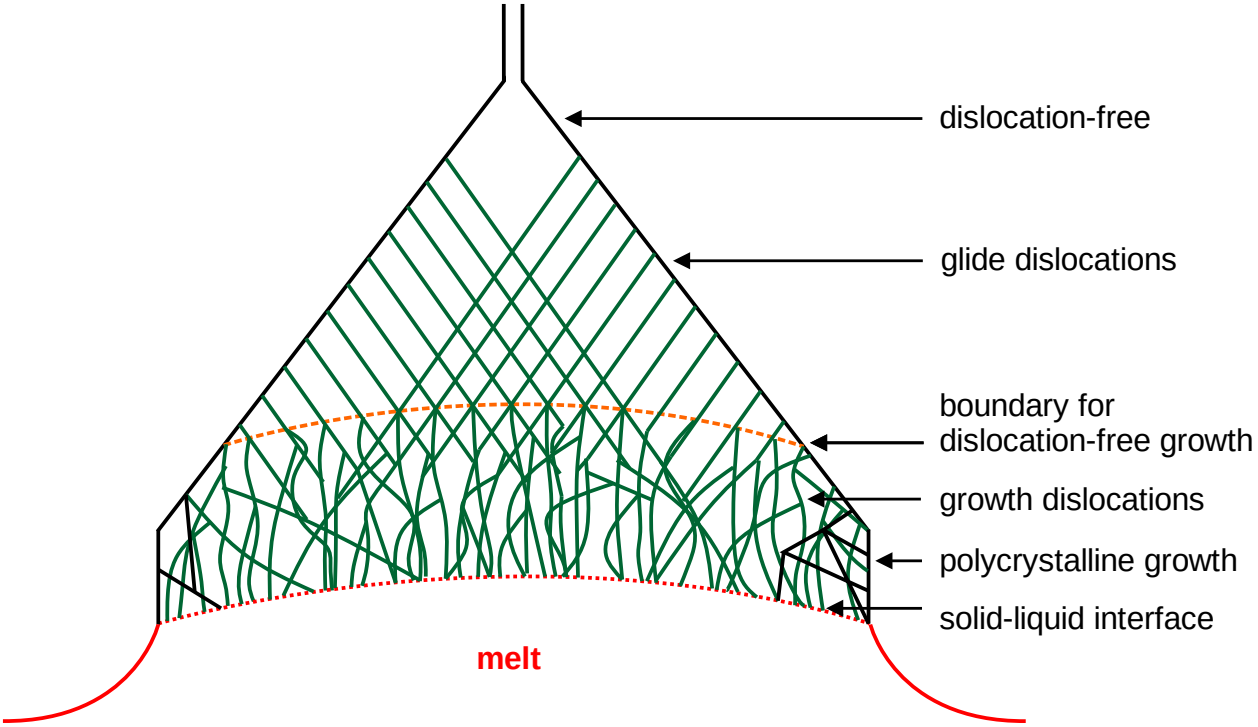

Fig. 3: Schematic drawing of dislocation propagation during the growth process of the top cone.

Seven crystals showing a growth ridge loss were selected to be cut into wafers and measured by XRT. An exemplary presentation of such characterization is shown in fig. 4 for one crystal. The increasing wafer diameter indicates the top cone phase. The XRT-images of wafers 1-4 in fig. 4 reveal contrasts of straight lines induced by the propagation of dislocations on their glide systems. Furthermore, these “glide dislocations” are only found on three sides of the crystal cone. Thus, the propagation is asymmetric. This was found to hold true for most crystals.

Starting with wafer 5 contrasts appear, which are not merely straight lines. Therefore, the assumption is made that glide as well as growth dislocations are present in the sample. No clear distinction is possible. When the dislocations density increases even further, small angle grain boundaries form causing polycrystalline growth. Polycrystalline growth can be distinguished by missing contrasts in the XRT-image due to a change of the diffraction conditions (see wafer no. 11).

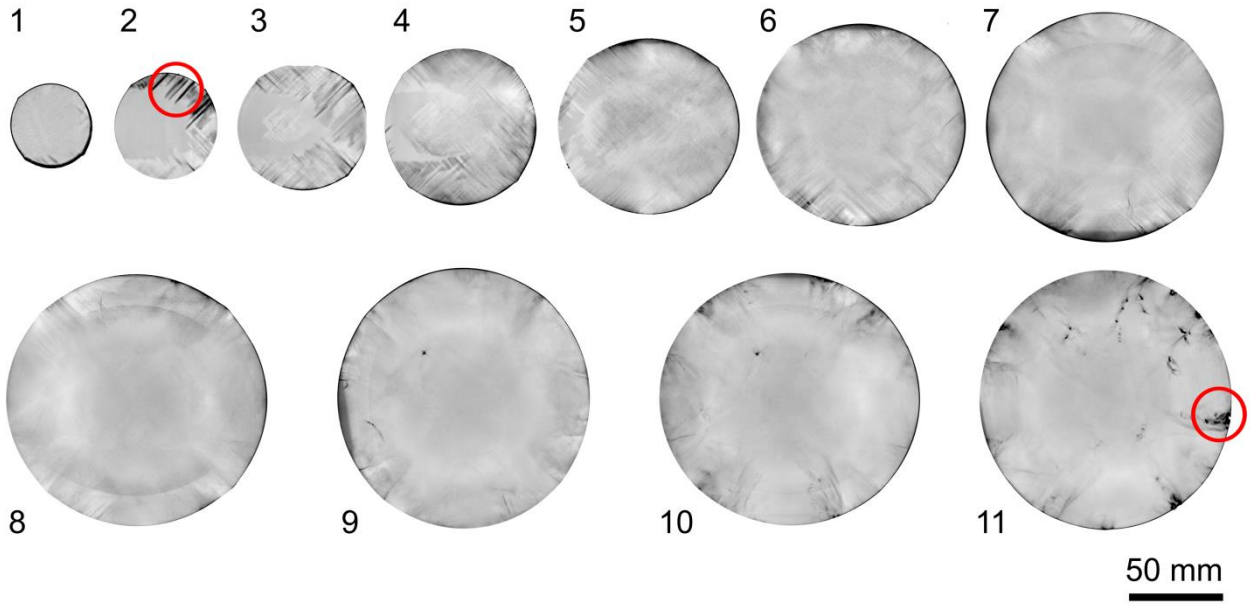

Fig. 4: XRT-images of wafers cut 10 mm apart from each other from a heavily As-doped CZ silicon crystal. The progress of the growth process is from wafer 1 to wafer 11. Wafers 1-8 are within the top cone and wafers 9-11 are from the body part of the crystal. Regions of glide dislocations and polycrystalline growth are marked exemplary on wafer 2 and wafer 11, respectively.

As shown in fig. 4, a classification of the patterns on the XRT-images in “dislocation-free”, “glide dislocations”, “growth + glide dislocations”, “growth dislocations” and “polycrystalline” is possible. The result of such classification of XRT-images taken from wafers of the top cones of seven crystals is shown in fig. 5. The growth progress is along the axis of the crystal diameter, from left to right.

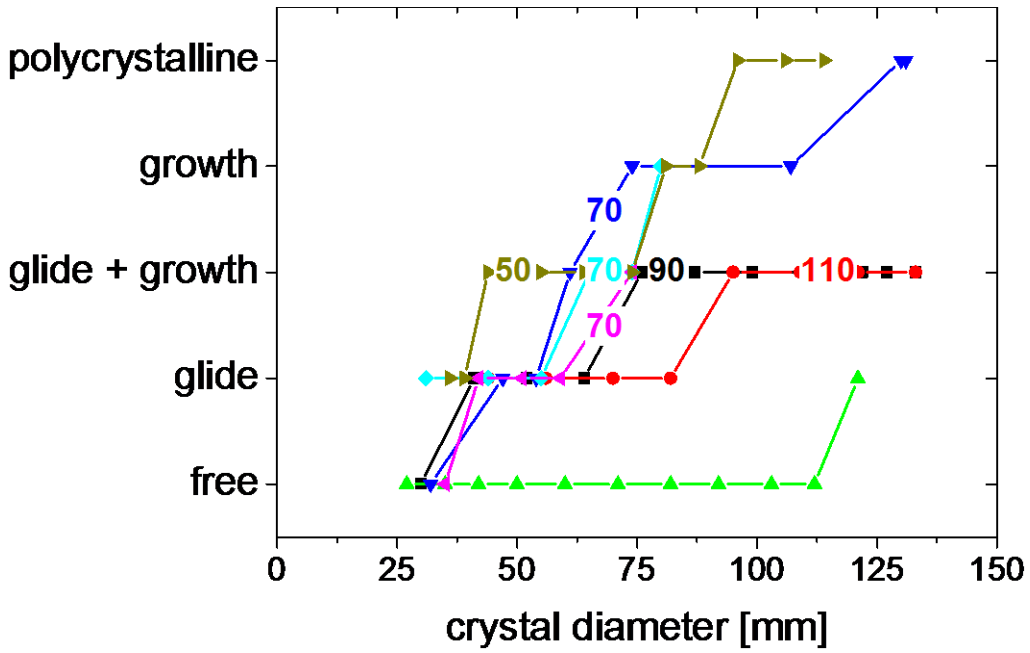

Fig. 5: Classification of dislocation patterns of XRT-images from wafers of seven heavily As-doped silicon crystals, where a growth ridge loss appeared. The numbers mark the diameter of the first occurrence of a growth ridge loss. The XRT-images of wafers 1-8 of fig. 4 compromise the red line with a growth ridge loss at a diameter of 110 mm.

As it can be seen in fig. 5, the crystals start as “dislocation-free” or with only “glide dislocations”, but not with “growth dislocations”. This confirms that the crystal growth process was dislocation-free at the beginning. Afterwards, “glide dislocations” appear followed by “glide + growth dislocations”. When no “glide dislocations” are visible any longer (see e.g. wafer 9 in fig. 4), only “growth dislocations” are dominant up to a point when “polycrystalline growth” can be recognized. Considering the different propagation mechanism of dislocations, it is presumed that the transition area between wafers with only “glide dislocations” and wafers with “glide + growth dislocations” marks the moment of the first appearance of dislocations during the growth process.

The numbers given in fig. 5 represent the crystal diameter where the first growth ridge loss has appeared. As it can be seen, the diameters of the occurrence of the first growth ridge loss correspond well to the appearance of the first wafer showing “glide + growth dislocations” in the XRT-images. Therefore, the formation of dislocations and the loss of a growth ridge coincide.

A XRT-image of a sample cut parallel to the growth direction is shown in fig. 6. The first growth ridge loss is marked by an arrow on the right-hand side. The dislocations can be traced back up to the first growth ridge loss and even beyond in the presumably formerly dislocation-free material. However, the resolution of the image is not sufficient to distinguish glide and growth dislocations.

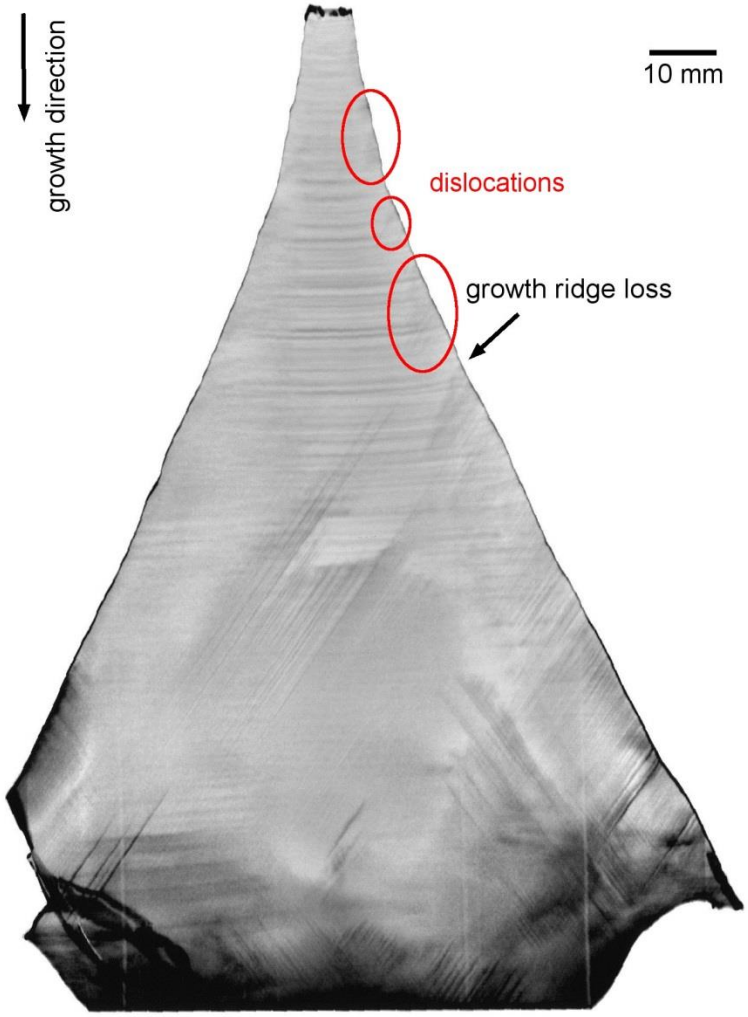

Fig. 6: XRT-image of a sample cut from a crystal with a growth ridge loss. Regions in the top of the cone with dislocations are marked separately. The arrow indicates the position of the first growth ridge loss. The dark contrast in the lower left side of the image originates from cracks in the sample.

To examine the growth ridges losses in more detail, samples containing a growth ridge loss were investigated by SXRT-measurements. The {660}-reflex of these SXRT-measurements of one sample are shown in fig. 7. The contrasts marked as “aligned

dislocations” in fig. 7 are aligned along <112>-directions and are most likely 60° dislocations with a burgers vector of ½ <110>, typical for misfit dislocations [20].

Since the dislocations affect the length of facets [9], it is possible to evaluate the X-ray contrasts related to dislocations by analyzing the length of facets (not shown here). The length of facets appearing inside of the growth ridge [8] was evaluated after defect selective etching of the SXRT sample under the optical microscope. Contrasts, depicted as “dislocation arrays” in fig. 7, did not affect the length of these facets. These “dislocation arrays” are most likely the result of an insufficient quality of sample preparation, whereas the appearance of the “aligned dislocations” reduced the length of the facets locally. Therefore, it can be concluded that only the “aligned dislocations” are present at the solid-liquid phase boundary during the growth process. But, it cannot be differentiated whether the “aligned dislocations” originate from the growth ridge loss or if the “aligned dislocations” reach the solid-liquid phase boundary from somewhere else and thus, affect the length of the facets.

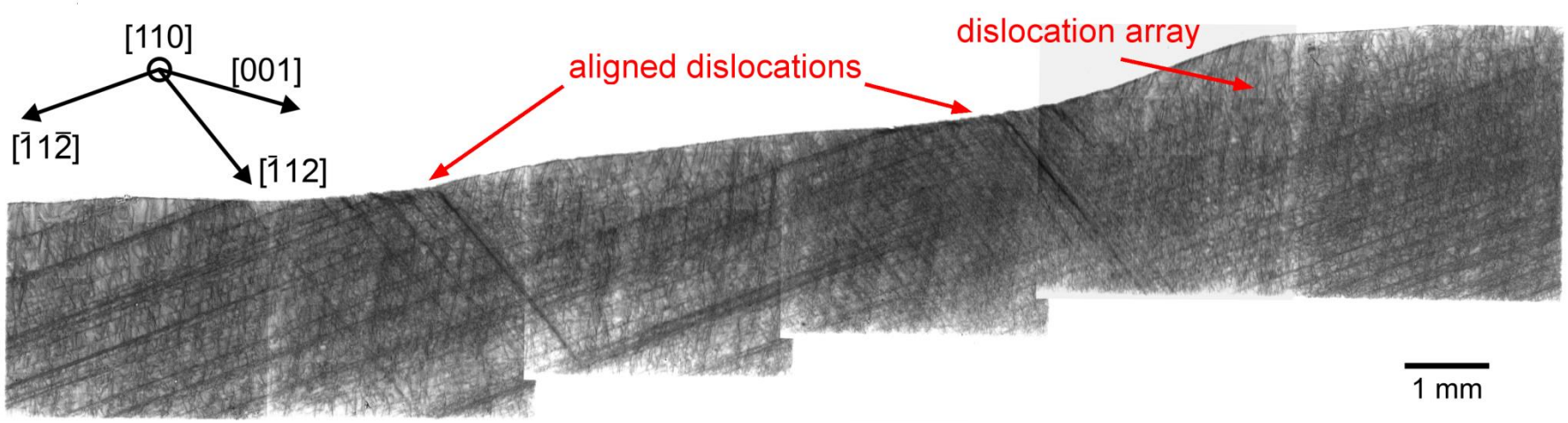

Fig. 7: SXRT (660)-reflex near the growth ridge loss. The top side of the sample represents the crystal surface. The growth direction is from left to right and marked by the [001]-direction. The appearances of "aligned dislocations" as well as "dislocation array" are highlighted by arrows.

4. Discussion

The following conclusions can be drawn from the results presented so far:

- Obviously, the dislocation origin is neither in the crystal body nor in the transition from the top cone to the crystal body.
- The dislocation origin was also not found to be in the thin neck, since the top wafers are either dislocation-free or compose solemnly of glide dislocations.
- The dislocation origin is during growth of the top cone.
- The asymmetric propagation of the glide dislocations in the before-hand dislocation-free crystal indicates the dislocation origin to be near the crystal edge. A dislocation origin in the crystal center would provoke a symmetric propagation of the glide dislocations.
- The crystal diameters of the first growth ridge loss and the crystal diameters of the first “glide + growth dislocations” correlate well. The growth ridges are lost one after another. A dislocation origin in the crystal center would have provoked all growth ridges to be lost at once.
- Dislocations depicted as “aligned dislocations” were present at the solid-liquid phase boundary, affecting the length of the facts and therefore the development of the growth ridge.

In summary, the authors conclude that it is highly likely for the origin of the first dislocations to be found near the crystal surface of the top cone or even in the vicinity of one of the growth ridges in the top cone.

These growth ridges compose of {111}-facets growing inside of the growth ridges [8; 16]. It could be possible that the facets are related to the formation of the dislocations. In literature it was shown that during the growth of InP the interruption of large facets led to the formation of twins [21; 22]. Although twin formation is a common phenomenon for III-V semiconductors [23–29], it is negligible for CZ growth of Si, since the risk for twinning is proportional to the ionicity and inverse proportional to the stacking fault energy [21; 30] and the stacking fault energy is highest in Si [30; 31]. Therefore, a more detailed view on the growth of these facets is necessary to clarify their influence on the risk of dislocation formation in heavily n-type doped Si.

5. Conclusion

In <100> oriented, heavily n-type doped silicon crystals grown by the Czochralski method dislocation forms frequently during growth of the top cone. The results from the XRT- and SXRT-measurements imply that the dislocation origin is near the growth ridges, which consist of {111}-facets. A further analysis is necessary to explain why dislocation formation took place near the growth ridges.

6. Acknowledgements

The authors want to thank Matthias Daniel and Kerstin Menzel, both from Siltronic AG, for providing the samples and performing the XRT-measurements.

Research and development published in this work were part of the projects *PowerOnSi* and *PowerBase*.

PowerOnSi with project number 100128500 was funded partly by the European Regional Development Fund (ERDF) and by the Saxony State Ministry for Science and Art (SMWK).

PowerBase has received funding from the Electronic Component Systems for European Leadership Joint Undertaking under grant agreement No 662133. This Joint Undertaking receives support from the European Union's Horizon 2020 research and innovation program and Austria, Belgium, Germany, Italy, Netherlands, Norway, Slovakia, Spain, United Kingdom.

7. References

[1] M. Grao Txapartegi and P. Gueguen, Status of the Power Electronics Industry 2015: Yole Developement

[2] R. Scala, M. Porrini and G. Borionetti, Growth and characterization of heavily doped silicon crystals, *Cryst. Res. Technol.* 46 (2011) (8), pp. 749–754

[3] K. M. Kim, Interface morphological instability in Czochralski silicon crystal growth from heavily Sb-doped melt, *J. Electrochem. Soc.: Solid-State Science and Technology* (1979), pp. 875–878

[4] T. Taishi, X. Huang, M. Kubota, T. Kajigaya, T. Fukami and K. Hoshikawa, Heavily doped boron silicon single crystal growth: Boron segregation, *Jap. J. Appl. Phy.* 38 (1999), pp. L223-L225

[5] T. Taishi, X. Huang, M. Kubota, T. Kajigaya, T. Fukami and K. Hoshikawa, Heavily boron-doped Czochralski (CZ) silicon crystal growth: segregation and constitutional supercooling, *Materials Science and Engineering B* 72 (2000), pp. 169–172

[6] H.-D. Chiou, Antimony concentration limitation in dislocation-free CZ silicon crystals, *Journal of Electrochemical Society* 152 (2005) (4), pp. G295-G298

[7] P. Rudolph, Handbook of Crystal Growth - Bulk Crystal Growth: Basic Techniques Volume II, Part A (2015), Elsevier

[8] T. F. Ciszek, Non-cylindrical growth habit of float zoned dislocation-free [111] silicon crystals, *J. Crys. Growth* 10 (1971) (3), pp. 263–268

[9] O. Weinstein and S. Brandon, Dynamics of partially faceted melt/crystal interfaces II: multiple step–source calculations, *J. Crys. Growth* 270 (2004) (1-2), pp. 232–249

[10] M. Weber, E. Gmeilbauer, R. Vorbuchner and A. Miller, Einkristallstab und Verfahren zur Herstellung desselben, Siltronic AG (2001), patent publication number DE10025870A1

[11] S. Soeta and S. Nakano, Method of manufacturing silicon single crystal (2015), patent publication number US 2015/0275392 A1

[12] P. Rudolph, M. Czupalla, B. Lux, F. Kirscht, C. Frank-Rotsch, W. Miller and M. Albrecht, The use of heater-magnet module for Czochralski growth of PV silicon crystals with quadratic cross section, *J. Crys. Growth* 318 (2011) (1), pp. 249–254

[13] Jordan Valley Ltd. (2017), http://www.jvsemi.com/, 3/16/2017

[14] A. N. Danilewsky, J. Wittge, A. Rack, T. Weitkamp, R. Simon, T. Baumbach and P. McNally, White beam topography of 300 mm Si wafers, *J. Materials Science: Materials in Electronics* 19 (2008) (S1), pp. 269–272

[15] F. S. d. Aragona, Dislocation etch for (100) planes in silicon, *J. Electrochem. Soc.: Solid-State Science and Technology* 119 (1972) (7), pp. 948–951

[16] V. V. Voronkov, B. Dai and M. S. Kulkarni (2011), Fundamentals and Engineering of the Czochralski Growth of Semiconductor Silicon Crystals. In: Comprehensive Semiconductor Science and Technology: Elsevier, pp. 81–169

[17] W. Zulehner, Czochralski growth of silicon, *J. Crys. Growth* 65 (1983), pp. 189–213

[18] A. Muiznieks, G. Raming, A. Mühlbauer, J. Virbulis, B. Hanna and W. von Ammon, Stress-induced dislocation generation in large FZ- and CZ-silicon single crystals--numerical model and qualitative considerations, *J. Crys. Growth* (2001) (230), pp. 305–313

[19] A. Lanterne, G. Gaspar, Y. Hu, E. Øvrelid and M. Di Sabatino, Investigation of different cases of dislocation generation during industrial Cz silicon pulling, *Phys. Status Solidi C* (2016), pp. 1–6

[20] R. Hull, J. C. Bean, L. Peticolas and D. Bahnck, Growth of GexSi1−x alloys on Si(110) surfaces, *Appl. Phys. Lett.* 59 (1991) (8), pp. 964

[21] M. Neubert, A. Kwasniewski and R. Fornari, Analysis of twin formation in sphalerite-type compound semiconductors: A model study on bulk InP using statistical methods, *J. Crys. Growth* 310 (2008) (24), pp. 5270–5277

[22] X. Li, R. Yang, F. Yang, T. Sun and N. Sun, Influence of the cone angle and crystal shape on the formation of twins in InP crystals, *Phys. Stat. Sol. (c)* 9 (2012) (2), pp. 165–168

[23] J. Amon, F. Dumke and G. Müller, Influence of the crucible shape on the formation of facets and twins in the growth of GaAs by the vertical gradient freeze technique, *J. Crys. Growth* 187 (1998), pp. 1–8

[24] H. Koh, M. Choi, I. Park and T. Fukuda, Twins in GaAs crystals grown by the vertical gradient freeze technique, *Cryst. Res. Technol.* 30 (1995), pp. 397–403

[25] J. Tower, R. Tobin, P. Pearah and R. Ware, Interface shape and crystallinity in LEC GaAs, *J. Crys. Growth* 114 (1991) (4), pp. 665–675

[26] V. Antonov, V. Elsakov, T. Olkhovikova and V. Selin, Dislocations and 90°-twins in LEC-grown InP crystals, *J. Crys. Growth* 235 (2002) (1-4), pp. 35–39

[27] H. Chung, M. Dudley, D. Larson Jr., D. Hurle, D. Bliss and V. Prasad, The mechanism of growth-twin formation in zincblende crystals new insights from a study of magnetic liquid encapsulated Czochralski-grown InP single crystals, *J. Crys. Growth* 187 (1998), pp. 9–17

[28] D. Hurle, A mechanism for twin formation during Czochralski and encapsulated vertical Bridgman growth of III-V compound semiconductors, *J. Crys. Growth* 147 (1995), pp. 239–250

[29] W. Bonner, InP synthesis and LEC growth of twin-free crystals, *J. Crys. Growth* 54 (1981) (1), pp. 21–31

[30] H. Gottschalk, G. Patzer and H. Alexander, Stacking fault energy and ionicity of cubic III-V compounds, *Phys. Stat. Sol. (a)* 45 (1978), pp. 207–217

[31] H. Föll and C. B. Carter, Direct TEM determination of intrinsic and extrinsic stacking fault energies of silicon, *Philosophical Magazine A* 40 (1979) (4), pp. 497–510